The developmental basis for the recurrent evolution of deuterostomy and protostomy

José M. Martín-Durán[1*], Yale J. Passamaneck[2,3], Mark Q. Martindale[2,3], Andreas Hejnol[1*]

[1]Sars International Centre for Marine Molecular Biology, University of Bergen, Thormøhlensgate 55, 5006 Bergen, Norway.

[2]The Whitney Laboratory for Marine Bioscience, University of Florida, 9505 Ocean Shore Blvd., St. Augustine, Florida 32080, USA.

[3]Kewalo Marine Laboratory, PBRC, University of Hawaii, 41 Ahui Street, Honolulu, Hawaii 96813, USA.

*Correspondence should be addressed to A.H. (andreas.hejnol@uib.no) or J.M.M.D. (chema.martin@uib.no)

The mouth opening of bilaterian animals develops either separate from (deuterostomy) or connected to (protostomy) the embryonic blastopore, the site of endomesoderm internalization. Although this distinction preluded the classification of bilaterian animals in Deuterostomia and Protostomia, and has influenced major scenarios of bilaterian evolution, the developmental basis for the appearance of these different embryonic patterns remains unclear. To identify the underlying mechanisms, we compared the development of two brachiopod species that show deuterostomy (*Novocrania anomala*) and protostomy (*Terebratalia transversa*) respectively. We show that the differential activity of Wnt signaling,

together with the timing and location of mesoderm formation, correlate with the differential behavior and fate of the blastopore. We further assess these principles in the spiral-cleaving group Annelida and propose that the developmental relationships of mouth and blastoporal openings are secondary byproducts of variations in axial and mesoderm development. This challenges the previous evolutionary emphasis on extant blastoporal behaviors to explain the origin and diversification of bilaterian animals.

In most animals, the precursor cells that form the inner tissues internalize at a specific site of the embryo in a process called gastrulation, which often involves the formation of a transient opening –the blastopore– that can later relate to the mouth and/or the anal openings[1]. The developmental connection of this transient blastoporal opening to the mouth (Fig. 1a) was typically used to divide bilaterally symmetrical animals (Bilateria) into Deuterostomia and Protostomia[2] (Fig. 1b), a node that recent molecular phylogenies strongly support[3,4]. In the traditional view, the mouth forms independently of the blastopore in Deuterostomia (literally, 'secondary mouth'), but is coupled to the blastoporal opening in Protostomia ('first mouth'), although tremendous variation in the blastoporal fate is seen in Protostomia[5,6] (Fig. 1b; Supplementary Table 1). Nearly all scenarios for bilaterian evolution presume the ancestral correspondence of the bilaterian blastoporal opening to the mouth of anthozoan cnidarians to explain the appearance of a tube-like alimentary canal with mouth and anus[7] (Fig. 1c). The amphistomy concept assumes that the ancestral pre-bilaterian condition was a 'Gastraea'-like organism with a single opening to the gut, which later formed a slit-like blastoporal opening that closed laterally with its ends forming the mouth and anus simultaneously[7-14]. Modifications of blastopore closure, e.g. by convergent extension[11], in this ancestral pattern of amphistomic gastrulation[7-10,12,13] would secondarily generate both deutero- and

protostomy (Fig. 1c). The planuloid-acoeloid scenario[15-17] deduces protostomy to be the ancestral mode of development in Bilateria, suggesting the secondary evolution of deuterostomy by a precocious formation of the mouth at the anterior area of the embryo and the formation of the anus from the blastopore[17-19] (Fig. 1c). Alternatively, deuterostomy could be the ancestral gastrulation mode in Bilateria[20,21], which is supported by its phylogenetic distribution[5] (Fig. 1b). If the behavior and fate of the transient blastoporal opening is important for understanding the evolution of Bilateria, knowledge of the exact developmental mechanisms underlying deuterostomy and protostomy is critical. In this regard, the striking presence of both modes of gastrulation in Protostomia (Fig. 1b), in particular between closely related species, can be used to understand the molecular and developmental basis for the recurrent evolution of deuterostomy and protostomy (Supplementary Table 1).

To identify the developmental basis of different blastoporal fates, we strategically selected two brachiopod species, *Novocrania anomala* and *Terebratalia transversa* (Supplementary Fig. 1a, j), on which previous experimental embryological work had been conducted[22,23] (Supplementary Fig. 2). Brachiopods are marine, sessile, filter-feeding invertebrates that belong to the clade Spiralia[3], which, together with the Ecdysozoa and Chaetognatha, form the Protostomia[3]. *N. anomala* and *T. transversa* share a comparable ecology and reproductive strategy (similar yolk-content, developmental timing, lecithotrophy, indirect life cycle), but display deuterostomic[22,24] and protostomic[23] development respectively (Fig. 1a). After fertilization, the embryos of these two brachiopod species undergo radial cleavage, gastrulation by invagination, and form a planktonic larva that eventually metamorphoses into the adult[22,23] (Supplementary Fig. 1). This exceptional case study allows us to exclude many

developmental variables that might influence gastrulation (e.g. yolk, egg size, cell number) and that often become significant when comparing blastoporal behaviors of embryos of distantly related and fast evolving lineages.

Results

Blastoporal dynamics

Classic embryonic labeling and cutting experiments revealed the opposing blastoporal fates of *N. anomala* and *T. transversa*[22,23] (Supplementary Fig. 2). In the deuterostomic *N. anomala*, the blastoporal opening moves and closes ventro-posteriorly (Fig. 1a; Supplementary Fig. 3a). During axial elongation, the ventral ectoderm is a compact, tightly packed cell layer, where cell proliferation (as seen by EdU incorporation) is widespread (Supplementary Fig. 3a). In the protostomic *T. transversa*, the blastoporal opening elongates anteroposteriorly (Supplementary Fig. 3a). The blastoporal opening closes mid-posteriorly, apparently by convergence of the ventral ectoderm[23], leaving the anterior end opened. Interestingly, increased EdU incorporation is observed in the anterior blastoporal rim during axial elongation in *T. transversa*, which is the region that internalizes first[23,25] potentially causing the elongation of the blastoporal opening[23] (Supplementary Fig. 3a). Importantly, our live-imaging recordings and cell-tracking analyses of gastrulation and axial elongation in *N. anomala* further exclude the possibility that cells from the blastoporal rim contribute to anterior/oral development (Supplementary Fig. 3b–d; Supplementary Videos 1–5). Blastopore closure appears to occur by proliferation and convergence of the blastoporal rim cells, and midline convergence does not appear to be a major morphological force at the ventral surface of *N. anomala* (Supplementary Fig. 3d; Supplementary Videos 3, 4). Therefore, morphological and cell-tracking evidences (Supplementary Fig. 3; Supplementary Videos 1–5), together with previous classic embryological studies[22,23] (Supplementary

Fig. 2a–d) indicate a blastoporal-independent origin of the mouth in *N. anomala*, reinforcing the suitability of these two brachiopod species to study the developmental basis of different blastoporal dynamics.

Axial and mesoderm development

To detect differences in the location and timing of appearance of the primary embryonic fates in *N. anomala* and *T. transversa* that might underlie the different relationships of the blastoporal rim to the formation of adult structures, we compared the expression of evolutionarily conserved molecular markers associated with the development of anterior, posterior and endomesodermal regions (Fig. 2; Supplementary Fig. 4; Supplementary Table 2). Initially, both brachiopod embryos express anterior markers (*six3/6*, *NK2.1*, *goosecoid* [*gsc*], *orthodenticle* [*otx*]) at the animal pole (Fig. 2a), the embryonic region that forms anterior ectodermal structures[22,23] (Supplementary Fig. 2). In the deuterostomic species *N. anomala*, these expression domains are always separate from the blastoporal rim, consistent with fate mapping, morphological and cell-tracking data (Supplementary Fig. 2c; Supplementary Fig. 3; Supplementary Videos 3–4). In the protostomic species *T. transversa*, however, *otx* and *brachyury* (*bra*) and later *six3/6*, *NK2.1* and *gsc* are also expressed on the side of the blastoporal rim that contributes to the mouth after axial elongation occurs (green arrows in Fig. 2a; Supplementary Fig. 4a, b). The posterior marker *even-skipped* (*evx*) is initially expressed encircling the vegetal pole of both embryos, as is *caudal* (*cdx*) in *T. transversa* (Fig. 2b). *N. anomala* retains this expression of *evx* and expands the expression of *cdx* around the blastoporal rim during development. However, the expression of these genes becomes restricted to the posterior blastopore lip as gastrulation begins in *T. transversa* (Fig. 2b). Therefore, the protostomic embryo undergoes an anteroposterior molecular re-patterning of the blastoporal rim before axial elongation and body plan formation.

No major differences related to endoderm formation (*foxA*, *GATA456* paralogs) are observed between either species (Supplementary Fig. 4a), but molecular differences coincident with the distinct mesodermal development reported for each brachiopod are evident (Fig. 2c; Supplementary Fig. 4a–c). While *N. anomala* internalizes the endomesoderm as a unit and later buds the mesoderm, which grows in a posterior-to-anterior direction[22,24], *T. transversa* segregates the mesoderm during gastrulation and the mesoderm grows in an antero-dorsal to posterior direction[26]. Accordingly, we first detect weak mesoderm expression (*twist* [*twi*] expressing cells) in the archenteron wall after gastrulation in *N. anomala*, and anterior mesodermal markers (*foxC*, *foxF*) appear ventrally, spatially separate from the blastoporal opening (Fig. 2c). In contrast, mesoderm (*twi* positive cells) is specified already at the blastula stage in *T. transversa*, with anterior mesodermal markers being expressed at the anterior blastoporal lip, on the side opposite of the domain that expresses posterior genes (Fig. 2c; Supplementary Fig. 4b), and ingresses earlier during axial elongation[23]. Thus, the anteroposterior re-patterning of the blastoporal rim together with the variation in mesoderm formation and patterning are the two developmental variables that co-vary with the differences in blastoporal fates in these two brachiopod species (Fig. 2d; Supplementary Fig. 4d).

Wnt pathway activity

Because endomesoderm specification and anteroposterior development are controlled by the canonical Wnt pathway in many previously studied animals[21,27], we hypothesized that differential activity around the blastoporal rim between the two brachiopod species might explain the observed variation in the deployment of anterior genes and the molecular patterning of the mesoderm. We thus treated embryos of *N. anomala* and *T. transversa* at different developmental stages with 1-azakenpaullone (Azk)

(Supplementary Fig. 5a), a selective inhibitor of GSK3-□[28] that has been shown to stabilize □catenin and over-activate the Wnt pathway in other systems. During cleavage, Azk treatment expands endodermal fates, inhibits ectodermal (both species) and mesodermal markers (*T. transversa* only), and abolishes gastrulation in both brachiopod species (Supplementary Fig. 5b, c), which is consistent with a conserved early role of □catenin in endomesoderm specification[21].

Azk treatment from blastula stages onwards in both *N. anomala* and *T. transversa* expands the expression of posterior genes (*evx*, *cdx*), and *axin* (*axn*), a read-out of the canonical Wnt pathway[29], and causes the reduction of anterior markers (*six3/6*, *NK2.1, gsc*, *otx*, *foxF*), including the loss of the anterior apical lobe in both embryos, and also the mantle lobe in *T. transversa* (Fig. 3a–d; Supplementary Fig. 6; Supplementary Fig. 7a; Supplementary Fig. 8). These data support a conserved role of the canonical Wnt pathway in inducing posterior fates[27]. As hypothesized, Azk treatment at the blastula stages inhibits the deployment of anterior genes (*six3/6*, *NK2.1*, *gsc*, *bra*) and an anterior mesodermal marker (*foxF*) around the blastoporal rim in the protostomic *T. transversa*, resulting in the extension of *evx* and *cdx* expression to the entire mesodermal and endodermal domains, respectively (Fig. 3c; Supplementary Fig. 6a, c; Supplementary Fig. 8a). Therefore, the canonical Wnt pathway influences the fate of different parts of the blastoporal rim by differentially regulating the axial patterning of the mesoderm and the expression of anterior/oral genes in *T. transversa*.

Surprisingly, treatment with Azk at the blastula stage neither prevents the ectodermal expression of *otx* on one side of the blastoporal rim, nor the restriction of *evx* and *cdx* to the opposite ectodermal side in *T. transversa* (Fig. 3c; Supplementary Fig. 6a; Supplementary Fig. 8a). The expression of *otx* in the anterior ectodermal blastoporal lip

disappears, however, in early Azk treated gastrulae, suggesting that *otx* has a late, Wnt-sensitive blastoporal rim expression in *T. transversa* (Supplementary Fig. 8c). Therefore, our findings indicate that signal(s) acting upstream and/or independently of the Wnt pathway at the blastula stage must trigger the primary asymmetric expression of *otx* and *evx*/*cdx* around the blastoporal rim of the protostomic *T. transversa*.

BMP pathway activity

We questioned whether these initial cues affecting the protostomic fate of the blastoporal opening in *T. transversa* could be related to the establishment of the dorso-ventral axis, and in particular to BMP signaling, as the blastoporal rim expression of *otx* in *T. transversa* occurs in the same region of expression of the BMP antagonist *chordin*[30] (*chd*) (Fig. 4a; Supplementary Fig. 4b), and *chd* also expands in Azk treated embryos (Supplementary Fig. 6c). Phosphorylation of SMAD1/5, the read-out of the BMP pathway[30], is first detected on one side of the blastula, and later, on the dorsal ectodermal side of both brachiopod species (Fig. 4a). Accordingly, *chd* and the ventral marker *netrin* (*ntr)* are expressed first in the gastral plate, and on the ectodermal ventral side after gastrulation (Fig. 4a). Thus, no differences in the expression and activity of BMP signaling core elements are observed between the two brachiopod species.

To discriminate the role of the BMP signaling during early brachiopod development and its impact on the different blastoporal fates of *N. anomala* and *T. transversa*, we treated embryos with the drug dorsomorphin homologue 1 (DMH1), a selective inhibitor of SMAD1/5 phosphorylation[31] and BMP activity (Supplementary Fig. 5a). In line with a conserved role of the BMP pathway in DV axis specification[30], DMH1 treatment induces the dorsal expansion of ventral ectodermal genes (*chd*, *ntr*) and ventrally expressed anterior ectodermal genes (*NK2.1*, *gsc*) in both brachiopod species (Fig. 4b,

c; Supplementary Fig. 7b; Supplementary Fig. 9). However, DMH1 treatment does not eliminate the re-patterning of the blastoporal rim in *T. transversa* (Supplementary Fig. 9a), although anterior ectodermal and mesodermal markers (*six3/6*, *NK2.1*, *gsc*, *otx*, *foxF*, *foxA*) are expanded and posterior fates (*evx*, *cdx*) are reduced in both brachiopods (Fig. 4b, c; Supplementary Fig. 9). Thus, the early expression of *otx* and *evx*/*cdx* on opposing sides of the blastoporal rim in the protostomic *T. transversa* occurs independently of the BMP pathway, which excludes a role of the dorsoventral axis in regulating the different blastoporal fates of the two brachiopod embryos, and suggests that the anteroposterior re-patterning of the vegetal pole in the protostomic species is regulated by earlier acting signals. Because the impairment of dorsoventral development affects anteroposterior patterning (Fig. 4b, c; Supplementary Fig. 7b; Supplementary Fig. 9), and vice versa (Supplementary Fig. 6c), our findings additionally suggest interplay between the specification of the anteroposterior (canonical Wnt pathway) and dorsoventral (BMP pathway) axes to regulate cell fates and body elongation along the primary axis in brachiopod embryos, as also observed in other bilaterian embryos[32-34], and in the specification of the oral-aboral and directive axes of cnidarians[35-37].

Blastoporal diversity in Annelida

To test whether the developmental principles we observed in brachiopods may explain the variation in the fate of the blastoporal opening in another bilaterian lineage, we examined the development of the annelid *Owenia fusiformis* and compared its development with available data from other annelids (Supplementary Fig. 10a; Supplementary Table 9). *O. fusiformis* is a member of the Oweniidae, the potential sister group of all remaining Annelida[38], whose members usually exhibit a highly stereotypical cleavage program referred to as quartet spiral cleavage[39]. In the closely related species *O. collaris*[40], the blastoporal fate has been described as being

deuterostomic. Our morphological analysis demonstrates that *O. fusiformis* forms a vegetal, round blastoporal opening during gastrulation, which moves only slightly along the animal-vegetal axis to end up in the anterior mouth. Therefore, *O. fusiformis* shows protostomous formation of the mouth (Supplementary Fig. 10d–h). Further analyses will be required to identify the exact origin of the anus.

We predicted based on our brachiopod data that anterior and posterior genes would be deployed in different sides of the blastoporal rim during gastrulation in the protostomic *O. fusiformis*, and that the way mesoderm develops may relate to the behavior of the blastoporal opening. Indeed, the anterior ectodermal genes *six3/6*, *NK2.1*, *gsc*, *otx*, the foregut marker *foxA*, and the posterior endo- and ectodermal genes *evx* and *cdx* are expressed on opposing sides of the blastoporal rim before axial elongation (Fig. 5a, b; Supplementary Fig. 11a). Mesodermal markers (*twi*, *bra*, *foxC*, *foxF* and *FoxL1*) suggest two distinct mesodermal populations (one anterior to the blastoporal rim and one posterior), which apparently expand as the embryo elongates antero-posteriorly (Fig. 5c). The short growth of the paired posterior mesodermal bands[40] (Supplementary Fig. 10f, g), likely related to a delayed formation of the definitive trunk in *O. fusiformis*[41], may explain the short axial elongation of the embryo, and thus the slight anterior move of the blastoporal opening (Supplementary Fig. 10e–g).

Discussion

By comparing two brachiopod species with opposing blastoporal fates, our findings help to illuminate the developmental basis for the recurrent evolution of deuterostomy and protostomy (Fig. 6). Although the nature of the primary developmental input(s) remains elusive, our results indicate that early signals repress Wnt activity on the ventral ectodermal side of the blastoporal rim in the protostomic *T. transversa* (Fig. 6).

This allows the expression of anterior ecto- and mesodermal genes in the ventral blastopore lip, which together with distinct dynamics of mesodermal morphogenesis[22-24,26], correlate with a behavior of the blastoporal opening different from that of *N. anomala* (Fig. 6; Supplementary Animation). Therefore, the different blastoporal fates observed in *N. anomala* and *T. transversa* may be caused by the differences in the modes and timing of axis specification and mesoderm development. Remarkably, our findings do not support a premature development of the mouth in *N. anomala* (Fig. 2a), as the planuloid/acoeloid scenario would imply[15-18]. Although the amphistomy concept[7-13] could conceptually explain the different blastoporal fates of *T. transversa* and *N. anomala*, our data do not show the proposed similar, but inverted, dynamics of blastopore closure between the two brachiopods (Supplementary Fig. 3; Supplementary Videos 1–5). Therefore, our study dissents on a mechanistic level from current scenarios for the evolution of deuterostomy and protostomy (Fig. 1c).

We further demonstrate that comparable developmental events to those observed in the protostomic brachiopod *T. transversa* may act in the protostomic annelid *O. fusiformis* (Fig. 5). Our data on this annelid are consistent with the reported expression of some of these genes in other protostomic polychaetes (Supplementary Table 9), but differ from *Capitella teleta*, whose blastoporal opening closes completely, and whose mouth forms later at a position anterior to the site of blastopore closure[42]. As it is also observed in the deuterostomous brachiopod *N. anomala*, the annelid *C. teleta* does not exhibit an overt anteroposterior patterning of the blastoporal rim[43-45] (Supplementary Table 9). Additionally, *C. teleta* displays a distinct mode of axial and precocious mesodermal development[46,47] with respect to other studied annelids and spiral-cleaving embryos[39] (Supplementary Table 9). Therefore, variation in axial and mesoderm development also correlates with modifications in the behavior of the blastoporal opening in annelids,

which solidifies the conclusions derived from the observations on brachiopod embryos. Our results together indicate that changes in the establishment of the axial identities and fate maps alone can explain the vast diversity of blastoporal behaviors observed in Spiralia.

Although the formation of a blastoporal opening during gastrulation is likely a homologous feature of cnidarian and bilaterian embryogenesis[21,48], its cellular composition, shape and later destination is dynamic during development and in evolution. Our study shows that distinct behaviors of the blastoporal opening appear to be influenced by changes in the fates of the cells that move over the blastoporal rim on their way to their final embryonic locations. Consequently, we propose that the shape and behavior of the blastoporal opening is a secondary effect of the embryonic architecture during gastrulation and axial elongation –commonly referred to as a 'spandrel' in evolutionary biology[49]. The cooption of the blastoporal opening – if still present – to a deuterostomic or protostomic fate in specific animal groups would thus correspond to secondary adaptations of this transient opening for the development of a digestive opening (the anus and the mouth respectively)[20] that have occurred independently multiple times during evolution, as the distribution of these characters in bilaterian phylogeny reveals (Fig. 1b). This scenario challenges the assumed value of extant blastoporal behaviours for explaining the evolutionary origin and diversification of Bilateria that has been presumed for over 100 years[4-7,9-11]. Freeing the constraint that the mouth and anus have a necessary association with the embryonic blastopore will help in understanding the developmental events underlying the evolution of an alimentary canal[5,20,21,50], and ultimately the appearance and diversification of bilaterian body plans.

Methods

Obtaining animals and embryos

Gravid adults were collected from the coasts near Friday Harbor Laboratories, U.S.A. (*Terebratalia transversa*), Espeland Marine Biological Station, Norway (*Novocrania anomala*), and Station Biologique de Roscoff, France (*Owenia fusiformis*) during their reproductive season (*T. transversa*: January; *N. anomala*: September; *O. fusiformis*: June and July), and spawned as previously described[22,23,40]. Embryos were collected at various stages of development up to late larval stage.

Drug treatments

Embryos of *N. anomala* and *T. transversa* were treated with either 0.5-10 □M 1-azakenpaullone (Azk) or 1-10 □M dorsomorphin homologue 1 (DMH1) diluted in seawater at different developmental stages (see Supplementary Fig. 5a for a detailed experimental setup). Solutions were changed every 24 h, and control conditions were performed with 0.1-1% dimethyl sulfoxide (DMSO). Treatments starting after fertilization were initiated on 2-cell stage embryos (approx. 2–3 h after sperm addition in both brachiopod species), to assure correct fertilization of the oocytes. Treatments on early blastula stages of *T. transversa* were performed at approx. 11 h post-fertilization, when the embryos are hollow spheres of blastomeres. Treatments on blastula stages (approx. 20 h post-fertilization in both brachiopod species) were conducted on mature blastulae, characterized by the presence of columnar cells with cilia, and the display of spinning/swimming behaviour. Treatments on gastrula stages were initiated as soon as the first signs of gastral plate invagination were evident (approx. 24 h post-fertilization in *T. transversa*). Once control embryos reached the desired developmental stage, control and treated embryos were fixed in 4% paraformaldehyde (PFA) for 1 h at room temperature, washed several times with 0.1% Tween-20 phosphate buffer saline (PTw),

and stored in methanol at -20 ºC (for gene expression analyses and phospho-SMAD1/5 antibody labelling) or PTw at 4 ºC (for actin labelling).

EdU labelling

Embryos of *N. anomala* and *T. transversa* at the required developmental stage were incubated in 100µM EdU diluted in sea water for 20 min and subsequently fixed in 4% PFA in sea water for 1 h at 4 ºC. Identification of EdU labelled nuclei was performed following manufacturer recommendations (Life Technologies). Embryos and larvae were cleared in benzyl benzoate/benzyl alcohol (2:1) before being scanned in a Leica SP5 confocal laser-scanning microscope. Image stacks were analysed with Fiji and Photoshop CS6 (Adobe). Brightness/contrast and colour balance adjustments were applied to the whole image, not parts.

Whole mount* in situ *hybridization.

Genes were identified from RNAseq data and gene orthologies were inferred by maximum likelihood analyses[51] (Supplementary Fig. S12). Single colorimetric *in situ* hybridization (ISH) of brachiopod and annelid embryos and larvae were performed following an established protocol[52]. Stained embryos and larvae were cleared in 70% glycerol and imaged with a Zeiss Axiocam HRc connected to a Zeiss Axioscope Ax10 using bright field Nomarsky optics. Double fluorescent whole mount *in situ* hybridization (DFISH) of *T. transversa* early gastrula was performed until first antibody incubation following the same protocol as for single colorimetric ISH. After the blocking step, samples were first incubated overnight at 4 ºC with an antibody anti-DNP POD conjugated (Perkin Elmer) diluted 1:100 in blocking solution. Samples were then washed in PTw and developed with TSA-Cy3 following the manufacturer's recommendations (Perkin Elmer). Before developing the second probe, remaining POD

activity from the antibody anti-DNP was quenched by incubating embryos with 1% oxygen peroxide diluted in PTw for 1 h at room temperature, followed by 10 min incubation at 67 ºC in 50% formamide, 2x sodium salt citrate (SSC), 1% SDS, 0.1% tween-20. After POD inactivation, samples were blocked in blocking solution for 1 h and incubated with antibody anti-DIG POD conjugated diluted 1:100 in blocking solution overnight at 4 ºC. After antibody washes with PTw, signal detection was performed with TSA-Cy5 as recommended by the manufacturer (Perkin Elmer). Fluorescently labelled embryos were cleared in benzyl benzoate/benzyl alcohol (2:1) before being scanned in a Leica SP5 confocal laser-scanning microscope. Image stacks were analysed with Fiji and Photoshop CS6 (Adobe). Brightness/contrast and colour balance adjustments were always applied to the whole image, not parts. Detailed *in situ* hybridization protocols are available upon request.

Actin labelling and immunohistochemistry

Brachiopod and annelid embryos were incubated with either BODIPY FL or Alexa647-conjugated phalloidin/phallacidin (Life Technologies) and Sytox Green or DAPI (Life Technologies) diluted in 1% bovine serum albumin (BSA) in 0.1% triton X-100 PBS for 1 h at room temperature to detect actin filaments and nuclei. Phosphorylated SMAD1/5 (pSMAD1/5) was detected on *N. anomala* and *T. transversa* embryos fixed and stored as for gene expression analyses. Before staining, embryos were gradually rehydrated to PTw, permeabilised in 0.2% tween-20, 0.2% triton X-100 PBS (PTwTx) and blocked in 1% BSA PTwTx for 1 h. Samples were incubated with antibody anti-pSMAD1/5 (Cell Signaling; ref. 9516) diluted 1:50 in 5% normal goat serum (NGS) in PTwTx overnight at 4 ºC, washed in 1% BSA PTwTx for 4 h, and the signal detected with an anti-rabbit Alexa647-conjugated antibody (Life Technologies) diluted 1:250 in 5% NGS in PTwTx. In all cases, embryos and larvae were cleared in benzyl

benzoate/benzyl alcohol (2:1) before being scanned in a Leica SP5 confocal laser-scanning microscope. Image stacks were analysed with Fiji and Photoshop CS6 (Adobe). Brightness/contrast and colour balance adjustments were applied to the whole image, not parts.

4D-microscopy

N. anomala embryos at the desired developmental stage were mounted under a 22x22 mm cover slide with clay feet on each corner. A gentle pressure was applied to the cover slide to immobilize the embryos, while still leaving enough space to develop normally. A Zeiss Ax10 Imager.M2 microscope with an internal focus drive was used to move the temperature-controlled stage to record the *z*-series. Pictures were captured with a SensiCam camera (PCO.Imaging), and compressed tenfold with a wavelet function (Lurawave, Germany). All recordings were performed at 12ºC with a 40x lens. Raw data is available upon request. The embryos recorded during blastula stage (Supplementary Video 1) and blastopore closure (Supplementary Video 4; Supplementary Video 5) were then removed from the microscope slide and placed in clean seawater to allow them recover. They were then fixed in 4% PFA as described above, and their morphology assessed by actin and nuclear labelling (Supplementary Fig. 3c). The embryo recorded during gastrulation (Supplementary Video 2) failed to proceed to normal axial elongation due to the mounting position. The embryo recorded during axial elongation (Supplementary Video 3) swam away during the recording and could not be recovered. Recordings were analysed as described elsewhere[53], using SIMIºBioCell software (SIMI, Germany). Time-lapse images were assembled into video recordings using Fiji, iMovie (Apple) and Photoshop CS6 (Adobe). The number of frames taken, the time between frames, and the number of focal levels per frame for each recording is as follows:

- *Recording 1 (Supplementary Video 1)*: 365 frames; 180 sec between frames; 30 focal levels; 2 µm increment. Total recorded time: 18 h and 15 min of development.
- *Recording 2 (Supplementary Video 2)*: 429 frames; 180 sec between frames; 25 focal levels; 1.7 µm increment. Total recorded time: 21 h and 27 min of development.
- *Recording 3 (Supplementary Video 3)*: 266 frames; 180 sec between frames; 30 focal levels; 1.3 µm increment. Total recorded time: 13 h and 18 min of development.
- *Recording 4 (Supplementary Video 4)*: 800 frames; 180 sec between frames; 25 focal levels; 1.8 µm increment. Total recorded time: 40 h of development.
- *Recording 5 (Supplementary Video 5)*: 373 frames; 180 sec between frames 1 and 239, and 360 sec between frames 361 and 373; 30 focal levels; 1.1 µm increment. Total recorded time: 25 h and 21 min of development.

Data availability

T. transversa, *N. anomala*, and *O. fusiformis* sequence data have been deposited in GenBank with the primary accession numbers KF946061–KF946084 and KR232531–KR232552). The original image stacks generated during 4D microscopy are available upon request.

Acknowledgements

We thank H. Hausen and O. Voecking for sharing the RNAseq data of *O. fusiformis* and expertise with the spawnings, B. C. Vellutini for help with collections and drug treatments, and G. S. Richards, F. Rentzsch, M. Iglesias and the members of the Hejnol laboratory for their comments on the manuscript. We also thank the staff at Friday

Harbor Laboratories, Espeland Marine Biological Station, and Station Biologique de Roscoff for assistance with animal collections. The study was funded by the core budget of the Sars Centre, and supported by The European Research Council Community's Framework Program Horizon 2020 (2014–2020) ERC grant agreement 648861 and a L. Meltzers Høyskolefond grant to A.H. J.M.M.D. was supported by Marie Curie IEF 329024 fellowship.

Author contributions

J.M.M.D. and A.H. conceived the project. J.M.M.D., Y.J.P. and A.H. performed animal collections and cloned genes, J.M.M.D conducted the experiments, and J.M.M.D. and A.H. performed the 4D recordings. Y.J.P. did the EdU analysis in *T. transversa*. J.M.M.D. and A.H. analyzed the data and wrote the manuscript, and Y.J.P. and M.Q.M. edited the paper. All authors discussed and commented on the data.

Competing financial interests

The authors declare no competing financial interests.

References

1 Gilbert, S. F. & Raunio, A. M. (Sinauer Associates, Inc., Sunderland, MA, 1997).

2 Grobben, K. Die systematische Einteilung des Tierreichs. *Verh. Zool. Bot. Ges. Wien* **58**, 491-511 (1908).

3 Dunn, C. W., Giribet, G., Edgecombe, G. D. & Hejnol, A. Animal Phylogeny and Its Evolutionary Implications. *Annu. Rev. Ecol. Evol. Syst.* **45**, 371-395 (2014).

4 Cannon, J. T. *et al.* Xenacoelomorpha is the sister group to Nephrozoa. *Nature* **530**, 89-93 (2016).

5 Martín-Durán, J. M., Janssen, R., Wennberg, S., Budd, G. E. & Hejnol, A. Deuterostomic development in the protostome *Priapulus caudatus*. *Curr. Biol.* **22**, 2161-2166 (2012).

6 Hejnol, A. & Martindale, M. Q. in *Animal Evolution: genes, genomes, fossils and trees* (eds M. J. Telford & D. T. J. Littlewood) 33-40 (Oxford University Press, 2009).

7 Sedgwick, A. On the origin of metameric segmentation and some other morphological questions. *Quart J Microsc Sci* **24**, 43-82 (1884).

8 Jägersten, G. On the early phylogeny of the Metazoa: the bilatero-gastrea theory. *Zool. Bidr. Uppsala* **30**, 321-354 (1955).

9 Remane, A. Die Entstehung der Metamerie der Wirbellosen. *Zool. Anz.* **14**, 18-23 (1950).

10 Arendt, D. & Nübler-Jung, K. Dorsal or ventral: similarities in fate maps and gastrulation patterns in annelids, arthropods and chordates. *Mech. Dev.* **61**, 7-21 (1997).

11 Steinmetz, P. R. H., Zelada-Gonzales, F., Burgtorf, C., Wittbrodt, J. & Arendt, D. Polychaete trunk neuroectoderm converges and extends by mediolateral cell intercalation. *Proc. Natl. Acad. Sci. U.S.A.* **104**, 2727-2732 (2007).

12 Arendt, D., Technau, U. & Wittbrodt, J. Evolution of the bilaterian larval foregut. *Nature* **409**, 81-85 (2001).

13 Nielsen, C. Evolution of deuterostomy - and origin of the chordates. *Biol Rev Camb Philos Soc* (2015).

14 Malakhov, V. V. New ideas on the origin of bilateral animals. *Russ J Mar Biol* **30**, S22-S33 (2004).

15 von Graff, L. *Die Organisation der Turbellaria Acoela*. (von Wilhelm Engelmann, 1891).

16 Hyman, L. H. *The Invertebrates. Vol II. Platyhelminthes and Rhynchocoela*. (McGraw-Hill, 1951).

17 Salvini-Plawen, L. On the origin and evolution of the lower Metazoa. *Zeitschr zool Syst Evol-forsch* **16**, 40-88 (1978).

18 Beklemishev, V. N. *Principles of Comparative Anatomy of Invertebrates*. (The University of Chicago Press, 1969).

19 Salvini-Plawen, L. v. Phylogenetischer Status und Bedeutung der mesenchymaten Bilateria. *Zool. Jb. Anat.* **103**, 354-373 (1980).

20 Lankester, E. R. Notes on the embryology and classification of the animal kingdom: comprising a revision of speculations relative to the origin and significance of the germ-layers. *Q. J. Microsc. Sci.* **s2-s17**, 399-454 (1877).

21 Martindale, M. Q. & Hejnol, A. A developmental perspective: changes in the position of the blastopore during bilaterian evolution. *Dev. Cell* **17**, 162-174 (2009).

22 Freeman, G. Regional specification during embryogenesis in the craniiform brachiopod *Crania anomala*. *Dev. Biol.* **227**, 219-238 (2000).

23 Freeman, G. Regional specification during embryogenesis in the articulate brachiopod *Terebratalia*. *Dev. Biol.* **160**, 196-213 (1993).

24 Nielsen, C. The development of the brachiopod *Crania* (*Neocrania*) *anomala* (O. F. Müller) and its phylogenetic significance. *Acta Zool.* **72**, 7-28 (1991).

25 Freeman, G. Regional specification during embryogenesis in Rhynchonelliform brachiopods. *Dev. Biol.* **261**, 268-287 (2003).

26 Long, J. A. & Stricker, S. A. in *Reproduction of marine invertebrates* (eds A. C. Giese, J. S. Pearse, & V. B. Pearse) 47-84 (Boxwood Press, 1991).

27 Petersen, C. P. & Reddien, P. W. Wnt signaling and the polarity of the primary body axis. *Cell* **139**, 1056-1068 (2009).

28 Kunick, C., Lauenroth, K., Leost, M., Meijer, L. & Lemcke, T. 1-Azakenpaullone is a selective inhibitor of glycogen synthase kinase-3 beta. *Bioorg. Med. Chem. Lett.* **14**, 413-416 (2004).

29 Jho, E. H. *et al.* Wnt/beta-catenin/Tcf signaling induces the transcription of *Axin2*, a negative regulator of the signaling pathway. *Mol. Cell. Biol.* **22**, 1172-1183 (2002).

30 De Robertis, E. M. Evo-devo: variations on ancestral themes. *Cell* **132**, 185-195 (2008).

31 Hao, J. *et al. In vivo* structure-activity relationship study of dorsomorphin analogues identifies selective VEGF and BMP inhibitors. *ACS Chem. Biol.* **5**, 245-253 (2010).

32 Fuentealba, L. C. *et al.* Integrating patterning signals: Wnt/GSK3 regulates the duration of the BMP/Smad1 signal. *Cell* **131**, 980-993 (2007).

33 Hashiguchi, M. & Mullins, M. C. Anteroposterior and dorsoventral patterning are coordinated by an identical patterning clock. *Development* **140**, 1970-1980 (2013).

34 Wei, Z., Range, R., Angerer, R. & Angerer, L. Axial patterning interactions in the sea urchin embryo: suppression of *nodal* by Wnt1 signaling. *Development* **139**, 1662-1669 (2012).

35 Genikhovich, G. *et al.* Axis Patterning by BMPs: Cnidarian Network Reveals Evolutionary Constraints. *Cell Rep.* (2015).

36 Leclère, L. & Rentzsch, F. RGM regulates BMP-mediated secondary axis formation in the sea anemone *Nematostella vectensis*. *Cell reports* **9**, 1921-1930 (2014).

37 Kraus, Y., Aman, A., Technau, U. & Genikhovich, G. Pre-bilaterian origin of the blastoporal axial organizer. *Nat Commun* **7**, 11694, doi:10.1038/ncomms11694 (2016).

38 Weigert, A. *et al.* Illuminating the base of the annelid tree using transcriptomics. *Mol. Biol. Evol.* **31**, 1391-1401 (2014).

39 Seaver, E. C. Variation in spiralian development: insights from polychaetes. *Int J Dev Biol* **58**, 457-467 (2014).

40 Smart, T. I. & Von Dassow, G. Unusual development of the mitraria larva in the polychaete *Owenia collaris*. *Biol Bull* **217**, 253-268 (2009).

41 Wilson, D. P. On the mitraria larva of *Owenia fusiformis* Delle Chiaje. *Philos. Trans. R. Soc. Lond. B Biol. Sci.* **221**, 231-334 (1932).

42 Eisig, H. Zur Entwicklungsgeschichte der Capitelliden. *Mittheilungen Aus Der Zoologischen Station Zu Neapel* **13**, 1-292 (1899).

43 Seaver, E. C., Yamaguchi, E., Richards, G. S. & Meyer, N. P. Expression of the pair-rule gene homologs *runt*, *Pax3/7*, *even-skipped-1* and *even-skipped-2* during larval and juvenile development of the polychaete annelid *Capitella teleta* does not support a role in segmentation. *EvoDevo* **3**, 8 (2012).

44 Boyle, M. J., Yamaguchi, E. & Seaver, E. Molecular conservation of metazoan gut formation: evidence from expression of endomesoderm genes in *Capitella teleta* (Annelida). *EvoDevo* **5**, 39 (2014).

45 Fröbius, A. C. & Seaver, E. C. ParaHox gene expression in the polychaete annelid *Capitella* sp. I. *Dev. Genes Evol.* **216**, 81-88 (2006).

46 Amiel, A. R., Henry, J. Q. & Seaver, E. C. An organizing activity is required for head patterning and cell fate specification in the polychaete annelid *Capitella teleta*: new insights into cell-cell signaling in Lophotrochozoa. *Dev. Biol.* **379**, 107-122 (2013).

47 Meyer, N. P., Boyle, M. J., Martindale, M. Q. & Seaver, E. C. A comprehensive fate map by intracellular injection of identified blastomeres in the marine polychaete *Capitella teleta*. *EvoDevo* **1**, 8 (2010).

48 Kraus, Y., Fritzenwanker, J. H., Genikhovich, G. & Technau, U. The blastoporal organiser of a sea anemone. *Current biology : CB* **17**, R874-876, doi:10.1016/j.cub.2007.08.017 (2007).

49 Gould, S. J. & Lewontin, R. C. The spandrels of San Marco and the Panglossian paradigm: a critique of the adaptationist programme. *Proc R Soc Lond B* **205**, 581-598 (1979).

50 Christiaen, L. *et al.* Evolutionary modification of mouth position in deuterostomes. *Semin Cell Dev Biol* **18**, 502-511 (2007).

51 Stamatakis, A. RAxML version 8: a tool for phylogenetic analysis and post-analysis of large phylogenies. *Bioinformatics* **30**, 1312-1313 (2014).

52 Hejnol, A. & Martindale, M. Q. Acoel development indicates the independent evolution of the bilaterian mouth and anus. *Nature* **456**, 382-386 (2008).

53 Hejnol, A. & Schnabel, R. What a couple of dimensions can do for you: Comparative developmental studies using 4D microscopy--examples from tardigrade development. *Integrative and comparative biology* **46**, 151-161 (2006).

Figure Legends

Figure 1. Fate of the blastopore and the evolution of Bilateria. (**a**) During deuterostomy, the blastoporal opening (bp; in blue) migrates from the vegetal pole to the posterior end and either closes (as in *N. anomala*; the anus opens around the red triangle) or forms the anus. The mouth (mo) forms anew. During protostomy, the blastoporal opening migrates anteriorly and becomes the mouth. The anus, if present, opens later. *T. transversa* lacks an anus. (**b**) The relation between the blastoporal, mouth and anal openings was traditionally used to split Bilateria into Deuterostomia and Protostomia, which is currently supported by molecular phylogenies. However, several lineages of Protostomia exhibit deuterostomic development, obscuring the ancestral mode of development for Protostomia (question mark). (**c**) The main scenarios for the evolution of Bilateria and the origin of a through gut presume the direct correspondence between the cnidarian mouth and the bilaterian blastopore. In the amphistomy scenario, elongation and mid closure of the blastopore (in blue) of the ancestral bilaterian ('Bilatero-gastraea') originated the mouth and anus (amphistomy). Subsequent variation during blastopore closure (small arrows) generated deuterostomy and protostomy. In the planuloid-acoeloid scenario, the blastoporal opening (in blue) of a planula-like ancestor formed the mouth (protostomy; curved arrow) of an acoeloid-like bilaterian. The anus evolved later and deuterostomy appeared as a precocious development of the mouth and the retention of the blastopore as anus. In each developmental stage in (**a**), left panels are lateral views and right panels are vegetal/ventral views. The asterisk denotes the animal/anterior pole. Drawings are not to scale. Scale bars in (**a**), 50 μm.

Figure 2. Gene expression during *N. anomala* and *T. transversa* embryogenesis. (**a**–**c**) Whole mount *in situ* hybridization of brachiopod embryos. (**a**) In both brachiopods, *six3/6*, *NK2.1*, *gsc* and *otx* are expressed in an anterior ectodermal domain. *six3/6* and

otx also exhibit anterior endomesodermal expression. In *T. transversa*, *otx* at gastrula and *six3/6*, *NK2.1* and *gsc* during early elongation are additionally expressed on the anterior/oral blastoporal rim. (**b**) In *N. anomala*, *evx* is expressed around the gastral plate (more intense in the future posterior side), blastoporal opening and posterior end; *cdx* is expressed on the presumably posterior side of the gastral plate and thereafter as *evx*. Both genes are expressed around the gastral plate in *T. transversa*, but become restricted to the posterior blastoporal rim and posterior larval tip after gastrulation. *cdx* is also expressed in the posterior endoderm. (**c**) *twi* is a general mesodermal marker in both brachiopods. In *N. anomala*, *foxC* and *foxF* are expressed in the ventral anterior mesoderm. In *T. transversa*, they are expressed in the anterior mesoderm lining the blastoporal opening, and later in more other putative mesodermal populations. In both brachiopods, *foxC* exhibits an anterior ectodermal domain. (**d**) Lateral drawings showing simplified expression domains of the analyzed markers. Only the ectodermal domain of anterior markers is drawn, the expression of endodermal and pan-mesodermal genes is shown just for the earliest stages, and only the anterior mesodermal domain of anterior mesodermal genes is shown in later stages. The different green intensities in *N. anomala* blastula and gastrula cartoons reflect the asymmetric expression of *cdx* and *evx* at these stages. The animal/anterior pole (asterisk) is to the top. The insets are vegetal/ventral views, except for *six3/6* and *NK2.1* (blastula/ gastrula; animal view) and *foxC* (blastula; animal view) of *N. anomala*. Upper insets of *foxC* and *foxF* in *N. anomala* are anterior views. Dashed circle in insets indicate the closing blastoporal opening in *N. anomala*. Green arrows point towards mouth expression, orange arrowhead towards endo-/mesodermal expression, and black arrowheads to ectodermal domains. bp, blastoporal opening; gp, gastral plate; mo, mouth.

Figure 3. Effect of 1-azakenpaullone in brachiopod embryos at blastula stage. (**a**) Whole mount *in situ* hybridization against *axin* (*axn*). In both brachiopods, *axn* is expressed in the gastral plate, stronger on the postero-dorsal side of the blastoporal rim, and in posterior territories. (**b**–**d**) The first column shows ventral views of control and treated embryos labeled with phalloidin (grey) and Sytox Green (nuclei; yellow). The second column is a schematic representation (lateral view) of control and treated embryos. The other columns are whole mount *in situ* hybridizations. Azk induces the loss of anterior structures, reduction of anterior markers (*six3/6*, *NK2.1*, *gsc*, *otx*, *foxF*), and expansion of posterior fates (*axn*, *evx*, *cdx*) in both brachiopods. In *T. transversa*, *evx* and *cdx* expands into meso- and endoderm respectively, but not around the whole blastoporal rim, which continues expressing *otx* on one side. In treated embryos, the blastoporal opening elongates and remains open opposite to the posterior tip of the embryo. The dashed line in (**c**) indicates probe trapping. The animal/anterior pole (asterisk) is to the top, and the insets are vegetal/ventral views, except in the treated embryo in (**c**) (lateral view). Green arrows point towards mouth expression, orange arrowhead towards endo-/mesodermal expression, and black arrowheads to ectodermal domains. al, apical lobe; bp, blastoporal opening; en, endoderm; em, endomesoderm; gl, gut lumen; me, mesoderm; ml, mantle lobe; mp, mesodermal pouches; mo, mouth; pl, pedicle lobe. Scale bars, 50 μm.

Figure 4. Dorsoventral development and effect of DMH1 in brachiopod embryos. (**a**) The first line shows lateral and dorsal views of immunostaining against phosphorylated SMAD1/5 (pSMAD1/5; grey) and Sytox Green (nuclei; red). The two lines below are whole mount *in situ* hybridizations. pSMAD1/5 appears first on one side of the blastulae, and later on the dorsal side of both brachiopod embryos (white arrowheads). Accordingly, *chd* and *ntr* are first expressed on the gastral plate (black

arrowhead), and later on the ventral side of the embryo (black arrowheads). (**b**, **c**), The first column shows ventral views of embryos labeled with phalloidin (grey) and Sytox Green (nuclei; yellow). The second column is a schematic representation (lateral view) of control and treated embryos. The third column shows dorsal views (except in treated *N. anomala*; lateral view) of immunostaining against pSMAD1/5 (gray; the staining in treated embryos in the surface epidermis is background) with Sytox Green (nuclei; red). The other columns are whole-mount *in situ* hybridizations. DMH1 treatment causes the loss of pSMAD1/5, the expansion of ventral ectodermal markers (*NK2.1*, *gsc*) and anterior markers (*six3/6*, *NK2.1*, *gsc*, *otx*, *foxF*), and the reduction of posterior fates (*evx*, *cdx*). The impaired posterior development affects blastopore closure in both brachiopods. The animal/anterior pole (asterisk) is to the top, and the insets are vegetal/ventral views, except in (**b**) control pSMAD1/5 (dorsal); *six3/6*, *NK2.1*, *gsc* treated *N. anomala* (anterior views); and the upper inset in *gsc* treated *T. transversa* (anterior view). Orange arrowheads point to endo-/mesodermal expression, and black arrowheads to ectodermal domains. al, apical lobe; bp, blastoporal opening; en, endoderm; em, endomesoderm; gl, gut lumen; me, mesoderm; ml, mantle lobe; mp, mesodermal pouches; mo, mouth; pl, pedicle lobe. Scale bars, 50 μm.

Figure 5. Gene expression during development of *O. fusiformis*. (**a**–**c**) Whole mount *in situ* hybridization. (**a**) *six3/6*, *NK2.1*, *gsc* and *otx* are expressed at the anterior blastoporal lip and in the mouth of the mitraria larva. *six3/6* is also expressed in the animal pole, *NK2.1* transiently in an animal/anterior domain during gastrulation and *otx* in the ciliated bands. (**b**) *evx* and *cdx* are expressed on the posterior side of the gastrula, first in the posterior endoderm, and then *evx* in the posterior larval ectoderm as elongation begins. *cdx* is also expressed in the hindgut and anus. (**c**) Mesodermal genes are not detected during gastrulation. *twi* is expressed in two lateral bands extending

from posterior to anterior, and in one antero-dorsal cell. *bra* is detected in the mesodermal cells that putatively form the trunk in the mitraria. *foxC* and *foxF* are expressed in the most anterior-lateral mesodermal cells and in a few cells in the anterior dorsal side of the embryo. In the mitraria, *foxC* and *foxF* are expressed in the posterior pharyngeal mesoderm. *foxL1* is expressed in the anterior portion of the mesodermal bands and in the lateral-posterior mesoderm of the pharynx. Mesodermal expression was assigned based on embryo and larval morphology (Supplementary Figure 10) and previous studies[40,41]. In all panels, the animal/anterior pole (asterisk) is to the top and the ventral side is to the left-bottom in gastrula and larval stages. Insets are vegetal/ventral views, except in blastula stages (animal views). Green arrows point towards mouth expression, orange arrowhead towards endo-/mesodermal expression, and black arrowheads to ectodermal domains. al, apical lobe; an, anus; bp, blastoporal opening; mo, mouth; pl, pedicle lobe.

Figure 6. The developmental basis of different blastoporal fates in *N. anomala* and *T. transversa*. Proposed model of the developmental control of fate of the blastoporal opening (bp, green dot) in the studied brachiopods. *N. anomala* specifies only posterior mesodermal fates around the blastoporal rim, which results in the coordinated movement of this opening to the posterior larval end. In the protostomic *T. transversa*, inferred early developmental inputs (F_x, in red) seem to restrict the activity of the Wnt pathway to the future posterior blastoporal lip, releasing the opposite side to deploy anterior ecto- and mesodermal fates. During axial growth, the blastoporal opening elongates and becomes co-opted into the mouth. The striped mesodermal areas in the early gastrula of *N. anomala* are prospective fates. The animal/anterior pole (asterisk) is to the top. al, apical lobe; bp, blastoporal opening; mo, mouth; pl, pedicle lobe. Drawings are not to scale.

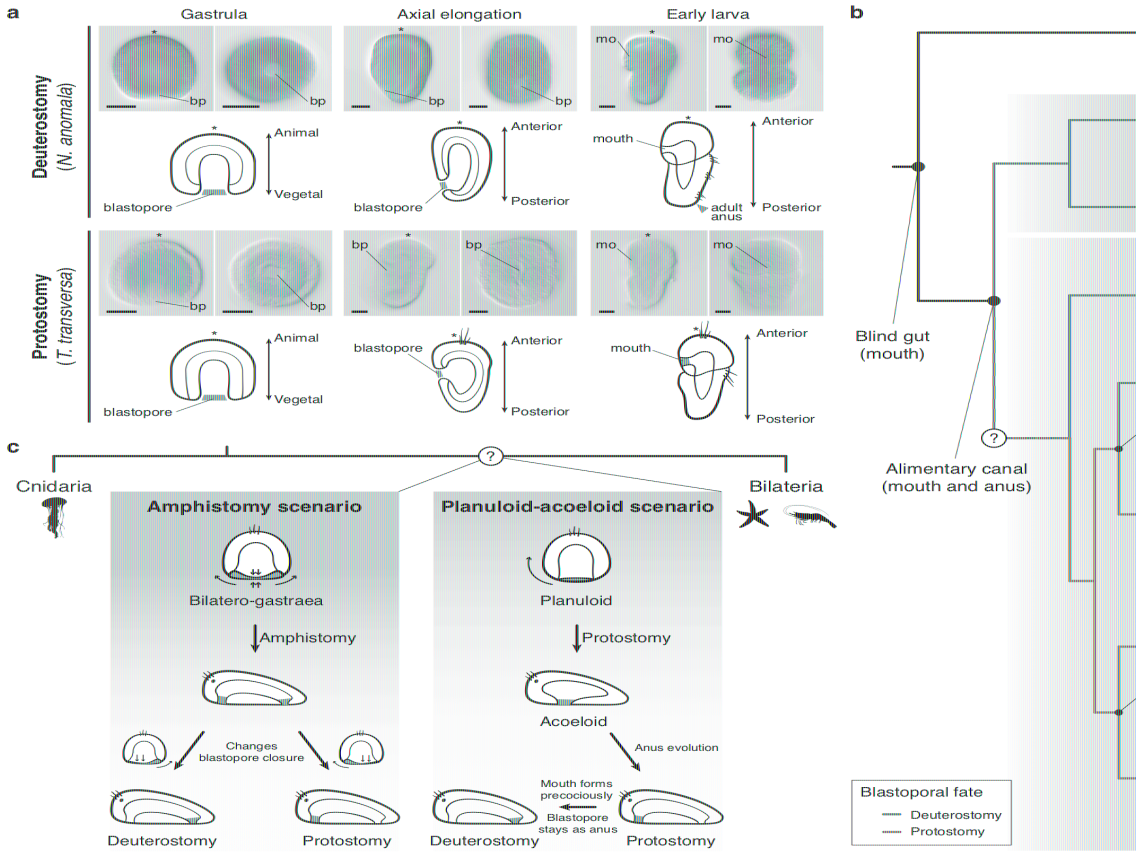
a
Gastrula
Axial elongation
Early larva
Deuterostomy
(N. anomala)
Protostomy
(T. transversa)
bp
mo
Animal
Vegetal
Anterior
Posterior
blastopore
mouth
adult anus
b
Blind gut
(mouth)
Alimentary canal
(mouth and anus)
Blastoporal fate
Deuterostomy
Protostomy
c
Cnidaria
Bilateria
Amphistomy scenario
Bilatero-gastraea
Amphistomy
Changes
blastopore closure
Deuterostomy
Protostomy
Planuloid-acoeloid scenario
Planuloid
Protostomy
Acoeloid
Anus evolution
Mouth forms
precociously
Blastopore
stays as anus
Deuterostomy
Protostomy

FIGURE 1

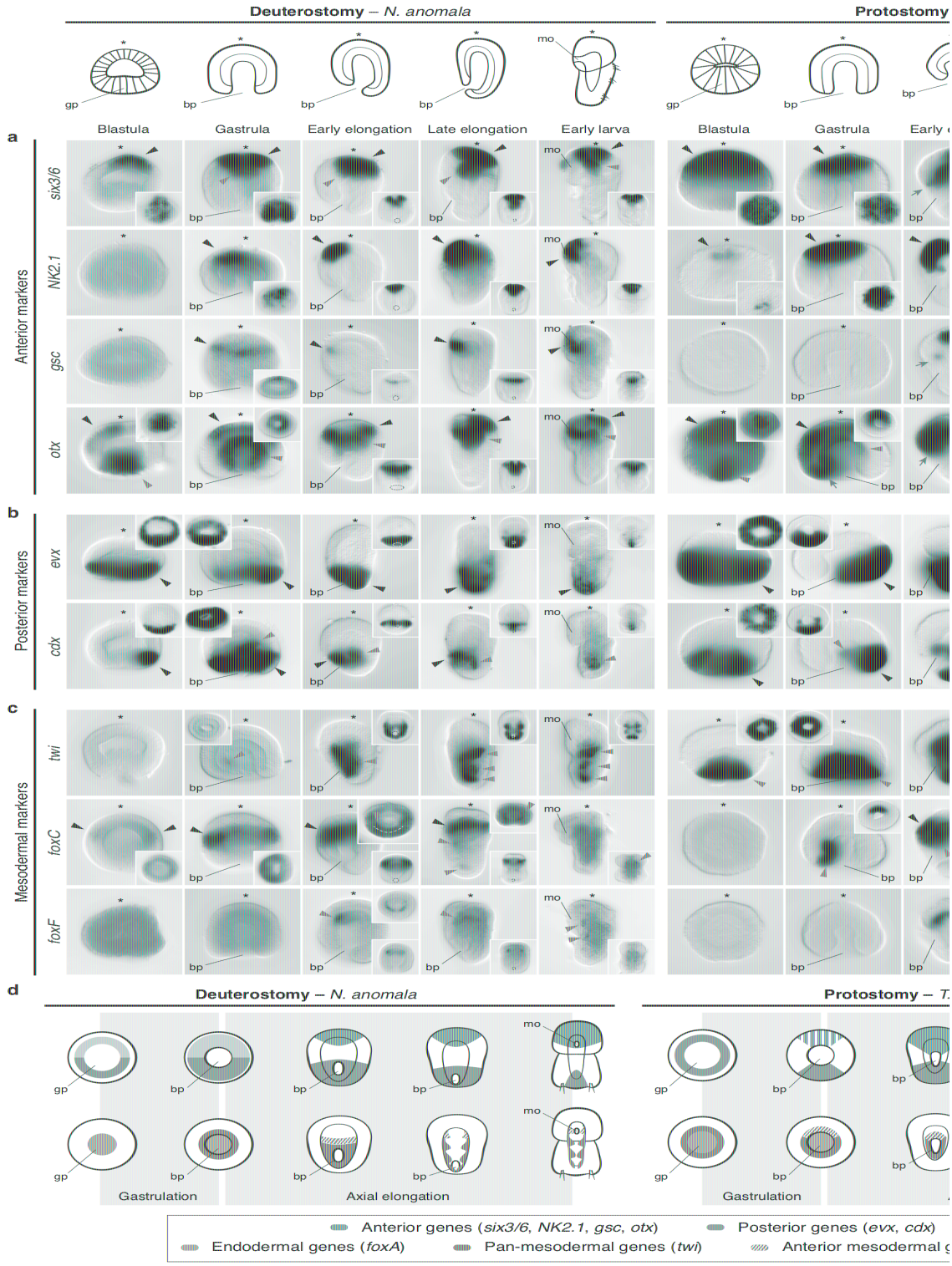
Deuterostomy – N. anomala
Protostomy
Blastula
Gastrula
Early elongation
Late elongation
Early larva
Blastula
Gastrula
Early
a
Anterior markers
six3/6
NK2.1
gsc
otx
b
Posterior markers
evx
cdx
c
Mesodermal markers
twi
foxC
foxF
d
Deuterostomy – N. anomala
Protostomy – T
Gastrulation
Axial elongation
Gastrulation
Anterior genes (six3/6, NK2.1, gsc, otx)
Posterior genes (evx, cdx)
Endodermal genes (foxA)
Pan-mesodermal genes (twi)
Anterior mesodermal
gp
bp
mo

FIGURE 2

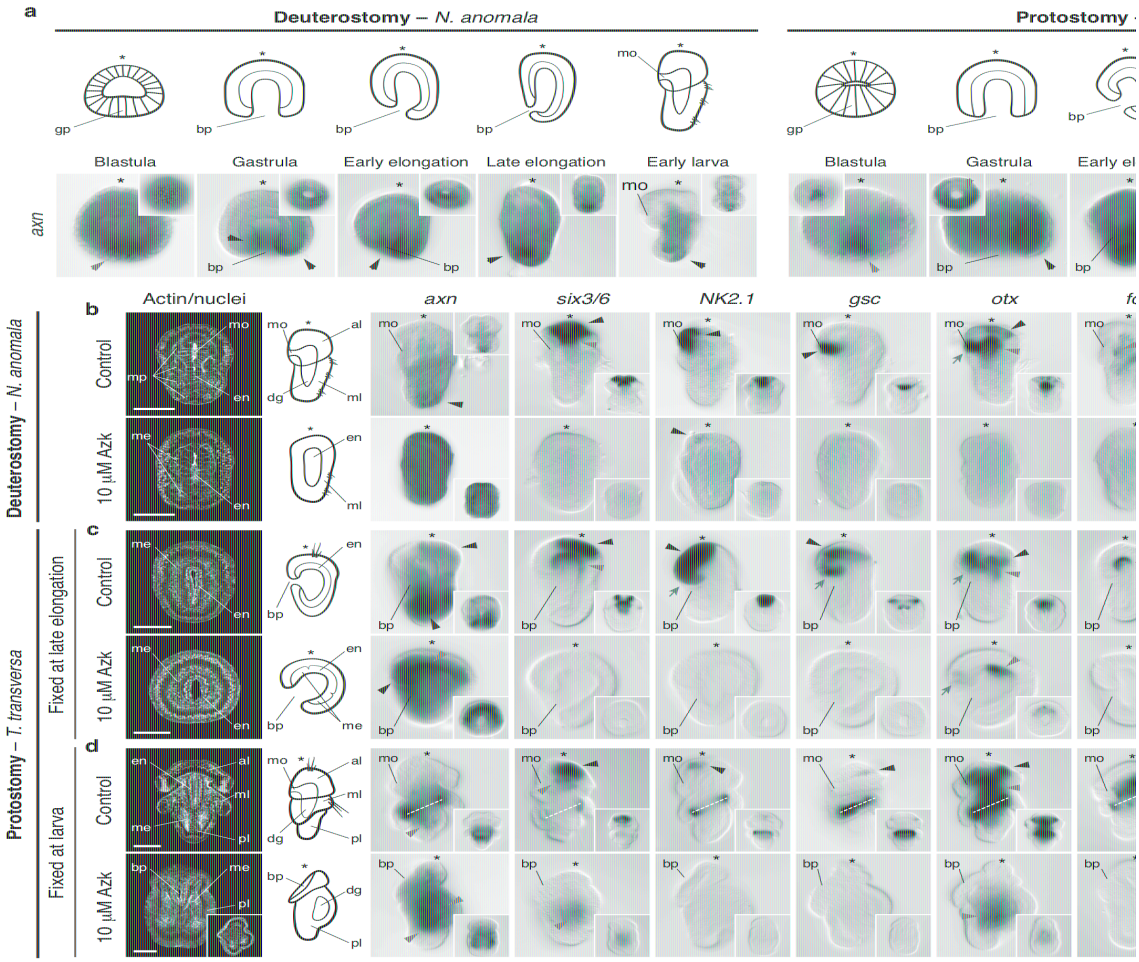
a
Deuterostomy – N. anomala
Protostomy
Blastula
Gastrula
Early elongation
Late elongation
Early larva
axn
b
Actin/nuclei
axn
six3/6
NK2.1
gsc
otx
Deuterostomy – N. anomala
Control
10 µM Azk
c
Fixed at late elongation
d
Fixed at larva
Protostomy – T. transversa
mo
al
ml
dg
pl
en
me
bp
gp

FIGURE 3

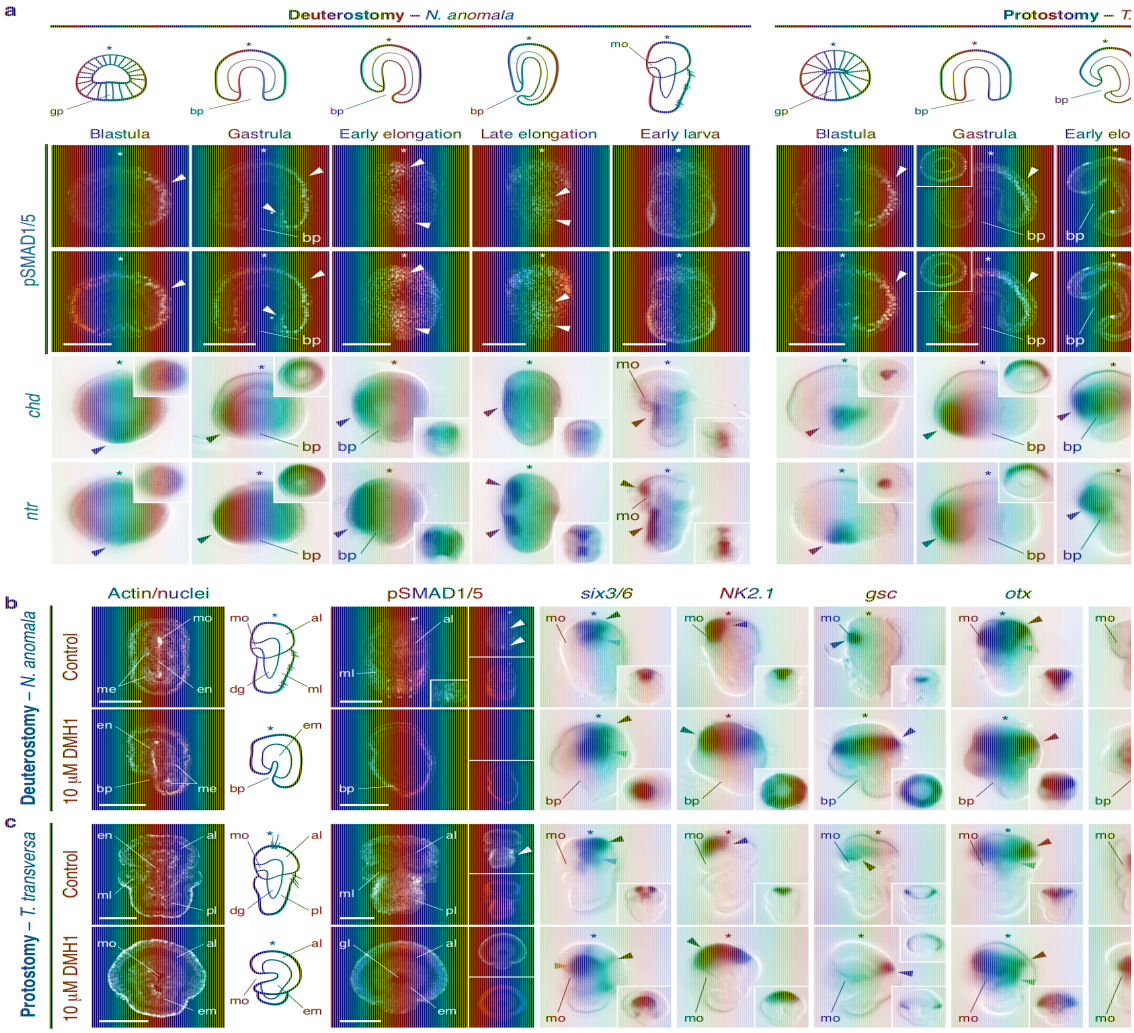
a
Deuterostomy – N. anomala
Protostomy – T.
Blastula
Gastrula
Early elongation
Late elongation
Early larva
Blastula
Gastrula
Early elo
pSMAD1/5
chd
ntr
gp
bp
mo
b
Actin/nuclei
pSMAD1/5
six3/6
NK2.1
gsc
otx
Deuterostomy – N. anomala
Control
10 μM DMH1
c
Protostomy – T. transversa
Control
10 μM DMH1
mo
al
me
en
ml
dg
em
pl
gl

FIGURE 4

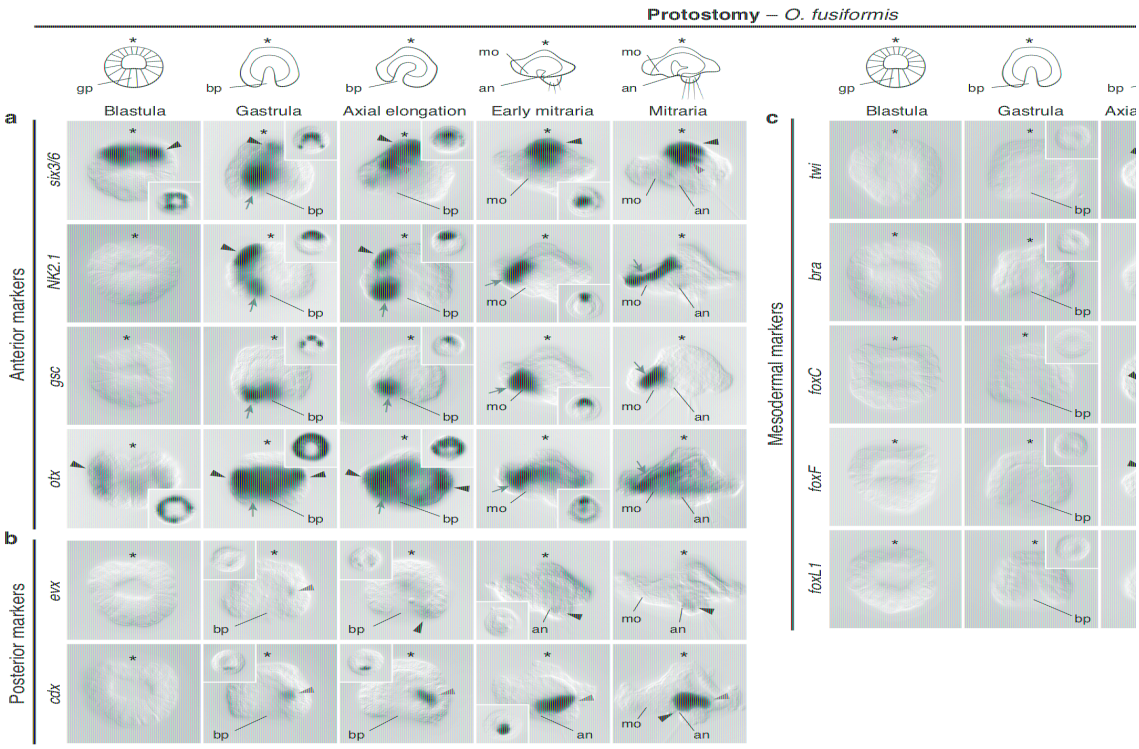
Protostomy – O. fusiformis
Blastula
Gastrula
Axial elongation
Early mitraria
Mitraria
a
Anterior markers
six3/6
NK2.1
gsc
otx
b
Posterior markers
evx
cdx
c
Mesodermal markers
twi
bra
foxC
foxF
foxL1
gp
bp
mo
an

FIGURE 5

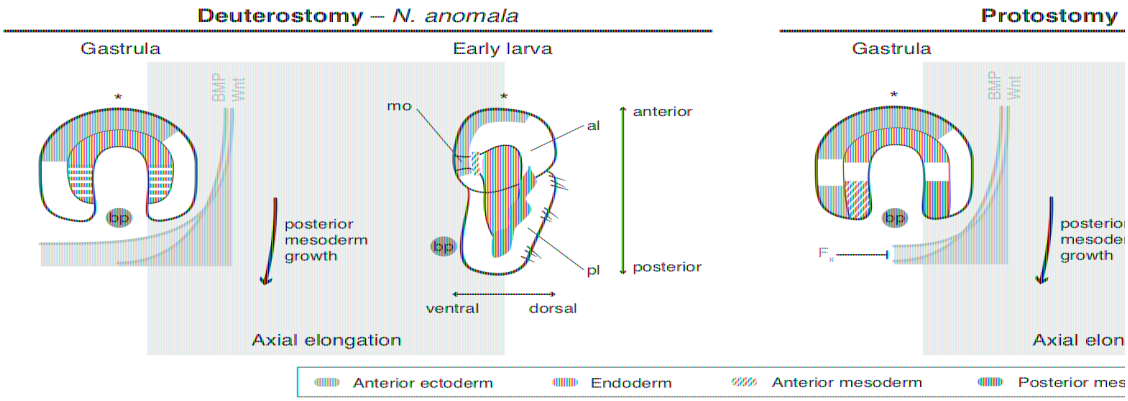
Deuterostomy – N. anomala
Protostomy
Gastrula
Early larva
Gastrula
BMP
Wnt
bp
posterior
mesoderm
growth
mo
al
pl
anterior
posterior
ventral
dorsal
Axial elongation
Axial elon
Anterior ectoderm
Endoderm
Anterior mesoderm
Posterior mes

FIGURE 6